

# The Metallurgical Structure of Electroless Nickel Deposits: Effect on Coating Properties

By R. N. Duncan

**A new phase diagram for electroless nickel alloys includes two non-equilibrium phases. The effect of structure on physical properties is described, including internal stress, magnetic response, ductility, corrosion resistance, passivity, porosity, hardness, wear resistance and strength.**

In the as-deposited condition, electroless nickel coatings can contain crystalline, micro-crystalline and amorphous phases. The relative amounts of these phases depend upon the formulation of the plating bath and upon the composition of the resulting deposit. These factors also determine the properties of the coating.

## Phase Diagrams

Phase or constitution diagrams are representations of the structures present in equilibrium in an alloy at different compositions and temperatures. They are used by metallurgists as road maps for alloy design, heat treatment, performance prediction, failure analysis, and the like. Most are binary, consisting of mixtures of only two elements.

Phase diagrams are normally developed by combining pure elements, melting the mixture at high temperature to homogenize it, then slowly cooling the alloy to room temperature. The formation of phases is then normally detected by thermal analysis, by X-ray diffraction, or by microscopic observation.

The phase diagram for nickel-phosphorus alloys was originally developed by Konstantinov in 1908<sup>1</sup>, many years before electroless nickel was discovered. It was modified by Hansen in 1943<sup>2</sup> and by Koeman and Metcalfe in 1958.<sup>3</sup> Part of this diagram is shown in Fig. 1.<sup>4</sup>

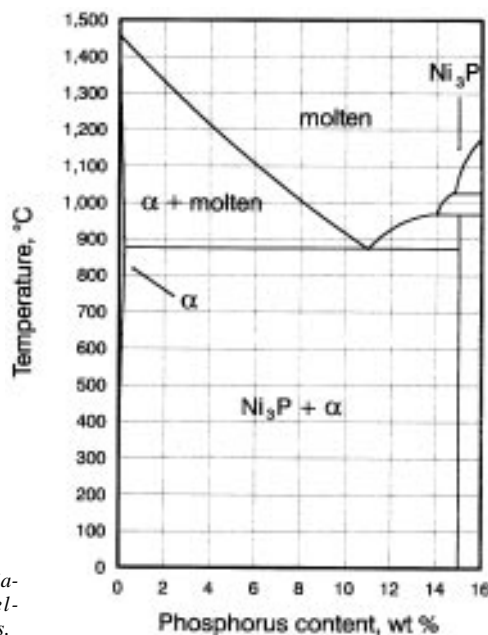


Fig. 1—Phase diagram for nickel-phosphorus alloys.

At temperatures below the melting point, the conventional diagram shows only two phases for alloys containing less than 15 percent phosphorus. There is a very small solid solution region called alpha ( $\alpha$ ), and the nickel phosphide,  $\text{Ni}_3\text{P}$ . The alpha phase consists of less than 0.17 percent phosphorus dissolved in nickel.  $\text{Ni}_3\text{P}$  is an intermetallic compound containing 15 percent phosphorus. The region between these two phases consists of a mixture of  $\alpha$  and  $\text{Ni}_3\text{P}$ .

This diagram has frequently been used to try to explain the structure of electroless nickel coatings. Different authors have theorized that  $\text{Ni}_3\text{P}$  and other phosphides were present in the as-deposited coating, and that the deposit consisted of a mixture of these intermetallic compounds with  $\alpha$  nickel.<sup>5,6</sup>

As-deposited electroless nickel coatings are not, however, in their equilibrium state. They are metastable and do not have the phases predicted by the traditional nickel-phosphorus phase diagram. This chart was prepared from alloys solidified from melts and applies only to alloys that have been exposed to high temperatures, such as heat-treated coatings. The traditional nickel-phosphorus diagram shows the coating to consist only of crystalline phases. Before heat treatment, however, most electroless nickel coatings consist largely of amorphous material.

To understand electroless nickel coatings and their properties, their non-equilibrium phases must be considered. To help with this understanding, a new phase diagram has been prepared that includes both the equilibrium phases produced after heat treatment and those metastable phases present in as-deposited coatings. This paper describes this diagram and its preparation and discusses how it can be used to predict the properties of electroless nickel coatings.

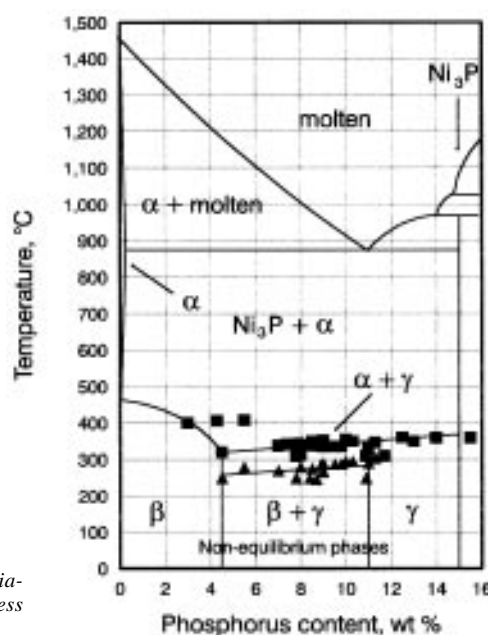


Fig. 2—Phase diagram for electroless nickel deposits.

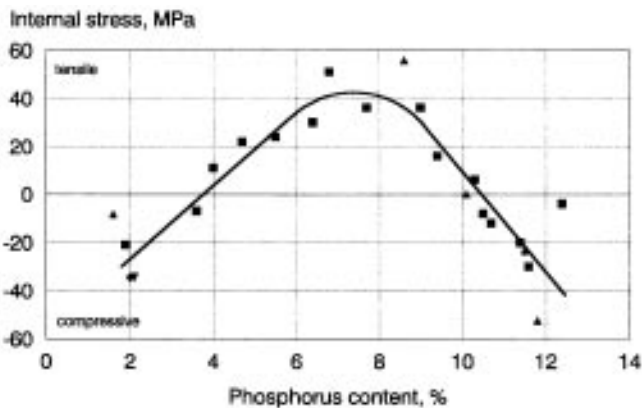


Fig. 3—Effect of phosphorus content on internal stress.

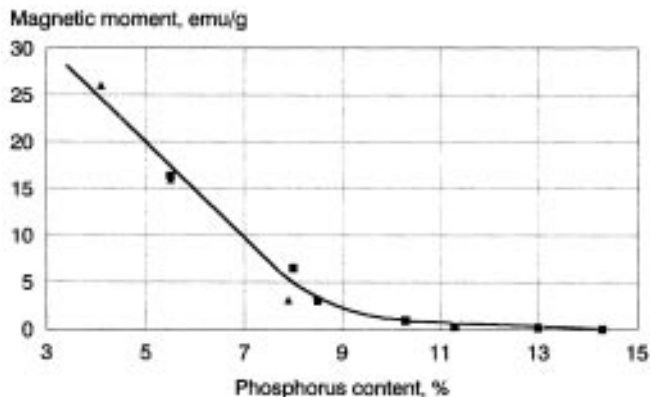


Fig. 4—Effect of phosphorus content on magnetic moment.

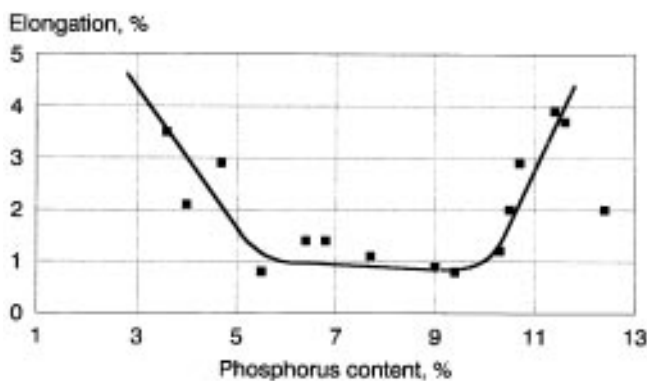


Fig. 5—Effect of phosphorus content on ductility.

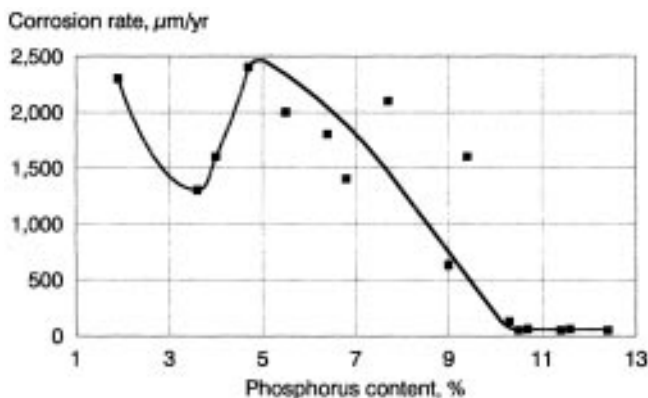


Fig. 6—Effect of phosphorus content on corrosion in 10% HCl.

### The Electroless Nickel Diagram

Phase changes in alloys can be determined in several ways. They can be identified directly by metallography or indirectly by observing changes in alloy properties. One simple technique, however, is differential thermal analysis. When a material changes state—from one phase to another—it either gives up or absorbs heat. By measuring this heat, phase changes and the temperature at which they occur can be detected. Because this method cannot identify the phase that has been produced, it must be supplemented by conventional diffraction measurements.

Several investigators have studied electroless nickel by this method. Researchers at General American Transportation probably conducted the first experiments when they measured the voltage between as-deposited and heat-treated coatings as they were heated in a molten lead bath.<sup>7</sup> Other tests have been conducted by Randin and Hintermann,<sup>8</sup> Smith,<sup>9</sup> Grewel,<sup>10</sup> Bagley and Turnbull,<sup>11</sup> Rajam,<sup>12</sup> Bozzini,<sup>13</sup> and Mallory.<sup>14</sup>

Other techniques for phase detection have included measuring alloy shrinkage<sup>15</sup> and magnetic moment,<sup>16</sup> as a function of temperature. Schemzel and Kreye carefully studied coatings containing 10 and 11.8 percent phosphorus, using electron diffraction to identify the different phases formed during heat treatment.<sup>15</sup> Graham, Lindsey and Read used X-ray diffraction to relate structure to phosphorus content and heat treatment.<sup>17</sup> Other X-ray diffraction studies were conducted by Kreye,<sup>18</sup> Crook,<sup>19</sup> Mahoney and Dynes,<sup>20</sup> and Martyak.<sup>21</sup> Investigations of the effect of composition on the properties of electroless nickel by Duncan<sup>22</sup> and by Weil and Parker<sup>23</sup> have tended to corroborate the structures observed by direct studies.

By combining the data from these different sources, a picture of the structure of electroless nickel coatings can be produced. This view is summarized in Fig. 2, which shows both the equilibrium phases present in traditional diagrams and the metastable phases predicted by more recent studies.

Before heat treatment, two additional phases are present, depending on the phosphorus content of the alloy. The first is the beta ( $\beta$ ) phase, which is a crystalline solid solution of phosphorus in nickel. It is similar to the alpha nickel phase shown on traditional diagrams, except that about 4½ percent phosphorus can be held in solution. The second phase is gamma ( $\gamma$ ), which is the totally amorphous phase that exists between approximately 11 and 15 percent phosphorus. Between the beta and gamma regions, a zone consisting of a mixture of  $\beta$  and  $\gamma$  phases is present.

Figure 2 is in good agreement with a theory proposed in 1962 by Moyseyev, based on theoretical considerations and x-ray diffraction results.<sup>24</sup> Moyseyev's hypothesis, however, placed the boundaries of the crystalline and glass-like phases at 5 and 8½ percent phosphorus, respectively.

The upper boundaries of temperature of the metastable phases are defined by two decomposition reactions. In the pure beta or pure gamma phases (*i.e.*, below 4 percent and above 11 percent phosphorus) only one reaction occurs—the conversion of the metastable phase to Ni<sub>3</sub>P and  $\alpha$ -nickel. With low phosphorus deposits, this reaction occurs at about 400 °C; with high phosphorus, it occurs at temperatures between 330 and 360 °C.

In the mixed  $\beta$  and  $\gamma$  phase region, a second decomposition reaction occurs at 250 to 290 °C. This reaction is the conversion of beta phase to  $\alpha$ -nickel, which results in precipitation of fine particles throughout the coating. When the tempera-

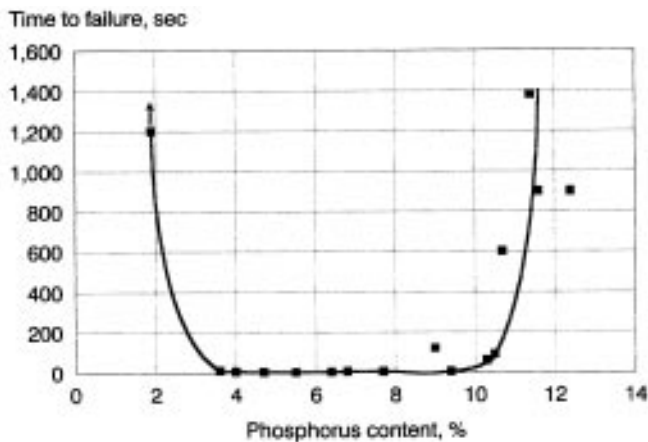


Fig. 7—Effect of phosphorus content on nitric acid resistance.

ture is increased to 310 to 330 °C, gamma (and any beta which may remain under non-equilibrium conditions) converts to  $\text{Ni}_3\text{P}$  and  $\alpha$ -nickel.

The boundaries between the regions in this new phase diagram cannot be precisely located because of the variation in the data used to construct it. This “shatter” is not unexpected, inasmuch as the diagram is based on the results of many different investigators.

#### Effect on Deposit Properties

Several authors have discussed the dependence of the properties of electroless nickel coatings on the phosphorus content of the deposit.<sup>17,22,23,25</sup> Some have even related this to deposit structure. The nature of this dependence becomes more apparent and understandable, however, when related to the phase diagram. For comparison, the effect of composition on the internal stress, magnetic response, ductility, corrosion resistance, passivity, porosity, hardness, wear resistance, and strength of electroless nickel coatings is shown in Figs. 3-11, respectively.

The boundaries between the beta, mixed  $\beta$  and  $\gamma$ , and gamma phase regions produce two transitions in most of the properties of electroless nickel coatings. This is most obvious with the intrinsic stress of the deposit.

As shown in Fig. 3,<sup>22,26-28</sup> below and above these transition concentrations, the internal stress of the coatings is compressive, while alloys with compositions between these values are tensile. Similarly, below about 7½ percent (where the amount of  $\beta$  and  $\gamma$  phase should be equal), stress increases approximately linearly by 14 MPa for every one-percent increase in phosphorus content. Above this value, it declines by an equal amount.

Probably the best known transition is that of magnetic response at 11 percent phosphorus. This is shown in Fig. 4.<sup>16,29</sup> At this concentration, when the coating becomes completely amorphous, its magnetic moment approaches zero and the deposit becomes non-magnetic. The magnetic susceptibility of deposits containing 11 percent phosphorus has been measured to be  $10^{-4}$  mks, which is similar to that of copper.<sup>30</sup> The magnetic response of low-phosphorus coatings has not yet been determined.

Ductility and internal stress seem to be related, as shown in Fig. 5.<sup>22</sup> High tensile stress appears to promote brittleness, but compressive stresses provide more flexible coatings. The highly stressed, mixed  $\beta$  and  $\gamma$  deposits have the lowest ductility, while the high-phosphorus gamma and low-phosphorus beta coatings have the best.

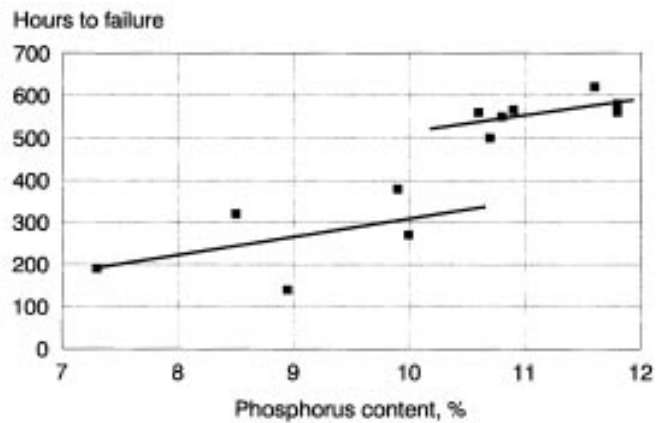


Fig. 8—Effect of phosphorus content on salt spray resistance.

The chemical corrosion of electroless nickel in hydrochloric acid and its passivity in nitric acid have many of the same trends as are seen with stress and ductility. These patterns are shown in Figs. 6<sup>22</sup> and 7,<sup>22</sup> respectively.

With beta alloys, acid corrosion declines with increasing phosphorus content until gamma forms at 4½ percent and corrosion begins to increase. As more phosphorus is added, however, and more gamma is formed, corrosion again declines, until at concentrations above 10½ percent, it stabilizes at 50  $\mu\text{m}/\text{yr}$ .

The passivity of electroless nickel in nitric acid is also greatly improved when a coating's phosphorus content is increased to more than 10½ percent. Little protection is obtained from mixed  $\beta$  and  $\gamma$  alloys. Very low-phosphorus  $\beta$  alloys are different from other coatings. They do not blacken, but instead develop a milky white color after one min.

Transitional behavior is also observed with salt spray resistance as is shown by Fig. 8.<sup>31</sup> With porosity, a step-type improvement in protection is obtained with gamma alloys. The performance of low-phosphorus  $\beta$  alloys is reported to be similar to that of medium phosphorus deposits.<sup>32</sup>

With hardness in the as-deposited condition, the transitions are also obvious, being the maximum and minimum values observed. This is summarized in Fig. 9.<sup>22</sup> Abrasive wear has a similar, but reciprocal, pattern as shown in Fig. 10.<sup>22</sup> Alloys that are totally beta phase provide the highest hardness and the lowest wear, while amorphous gamma alloys have the reverse properties.

The strength of electroless nickel deposits is shown in Fig. 11.<sup>23,33</sup> This curve has the same maximum and minimum pattern as hardness and wear. Low-phosphorus beta alloys are weak, with strengths much less than that of pure nickel. The strength of highly stressed, mid-phosphorus alloys, containing large amounts of  $\gamma$  in beta phase, is as high as many tool steels. Once the coating becomes fully amorphous, however, its strength declines.

#### Why Structure Affects Properties

The transitions in the properties of an electroless nickel coating are most likely the result of changes in the structure of the deposit that occur as its phosphorus content is changed. About 4½ percent is the maximum amount of phosphorus which can be held in solid solution at 90 °C by crystalline beta phase. Once the bulk concentration of the deposit exceeds this quantity, the excess phosphorus is rejected by the beta phase and forms  $\gamma$  phase at the boundaries between beta grains. As the bulk concentration is increased further, the

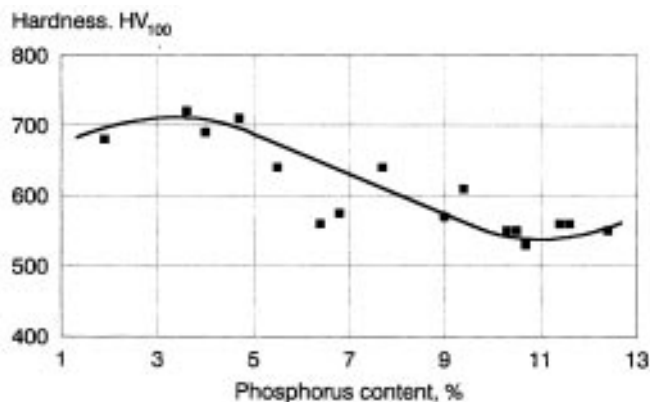


Fig. 9—Effect of phosphorus content on hardness.

amount of  $\gamma$  also increases, while  $\beta$  decreases, until at 11 percent, the alloy becomes totally composed of gamma.

When the coating is either completely beta or gamma, it is in its most homogeneous state. In this condition, it is compressively stressed and most ductile. When a mixture of the two phases is present, a structural mismatch probably exists between them, causing tensile stresses and brittleness. This mismatch is most severe after the first transition, when the amount of gamma is quite small. The deposit's hardness and wear resistance is also affected by this condition. Maximum hardness and minimum wear occur when gamma first appears, while the opposite occurs when the beta phase disappears.

Similarly, the coating is in its most passive and fully corrosion-resistant state when it is composed only of gamma phase. When only crystalline beta phase is present, its level of corrosion in hydrochloric acid is similar to that of unalloyed nickel, about 2000  $\mu\text{m}/\text{yr}$ .<sup>34</sup> Raising the phosphorus content of the beta phase improves its corrosion resistance, but not its passivity.

Once the phosphorus concentration is increased to more than about 4<sup>1</sup>/<sub>2</sub> percent, and gamma phase begins to form, corrosion is again increased. The mixture of the two phases, with two different compositions, probably produces active/passive corrosion cells within the alloy, causing it to suffer severe chemical attack. This is similar to the loss of corrosion resistance that occurs after coatings are hardened.<sup>35</sup>

The phase diagram also explains why various electroless nickel alloys harden differently. Low- and high-phosphorus alloys can experience only one decomposition reaction to  $\alpha$  phase and Ni<sub>3</sub>P. Because this reaction does not occur until the temperature is raised above 330 °C, hardening cannot start until this point is reached. Mixed  $\beta$  and  $\gamma$  alloys, however, experience a second decomposition reaction—to  $\alpha$  and  $\gamma$ —at temperatures between 260 and 280 °C. Accordingly, these coatings begin to harden earlier and at lower temperatures than either pure beta or gamma alloys.

#### Summary

Electroless nickel plating solutions are formulated with different chemicals and for different objectives. Some are designed to provide coatings with specific properties, while others are intended to be easy to operate, or to have a high deposition rate, or to have a long life.

While all are valid goals for formulation, they result in coatings with widely varying compositions. Their phosphorus content may range from 1 to 13 percent, and their structure may vary from pure crystalline beta phase to totally amor-

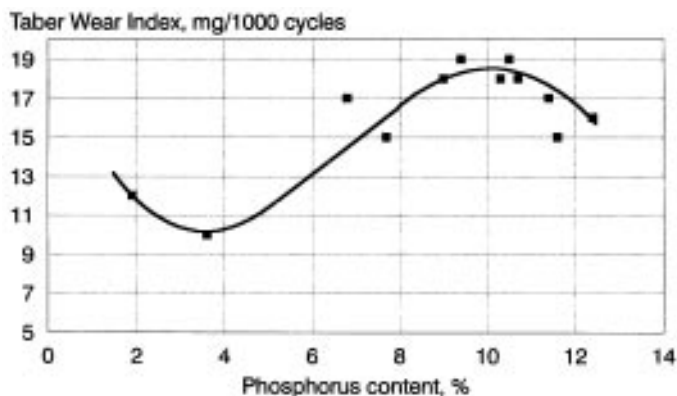


Fig. 10—Effect of phosphorus content on wear.

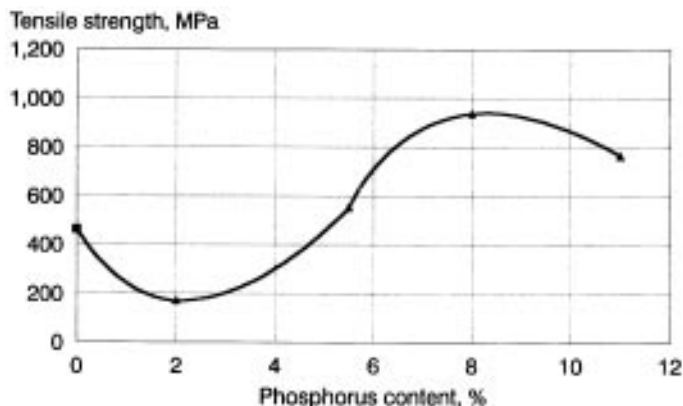


Fig. 11—Effect of phosphorus content on tensile strength.

phous gamma phase. These variations have a marked effect upon many properties of the coating.

**Editor's note:** Manuscript received, May 1995; revision received, August 1996.

#### References

1. N. Konstantinov, *Z. Anorg. Chem.*, **60**, 405 (1908).
2. M. Hansen, *Der Aufbau der Zweistofflegierungen*, Edwards Brothers, Ann Arbor, MI 1943.
3. J. Koeman and A.G. Metcalfe, *Trans. Metallurg. Soc. of AIME*, 571, (Aug. 1958).
4. H. Baker, ed., *ASM Handbook, Vol. 3, Alloy Phase Diagrams*, 2-313, ASM International, Metals Park, OH (1992).
5. G.G. Gawrilov, *Chemical (Electroless) Nickel Plating*, Portcullis Press Ltd., Redhill, England, 1979; p. 101.
6. W. Riedel, *Electroless Nickel Plating*, ASM International, Metals Park, OH, 1991; pp. 68-69.
7. A.W. Goldstein, W. Rostoker, F. Schossberger and G. Gutzeit, *J. Electrochem. Soc.*, **104**(2), 104 (1957).
8. J.P. Randin, P.A. Maire, E. Saurer and H.E. Hinterman, *ibid.*, **114**(5), 442 (1967).
9. D.D. Smith, *Thermal Conductivity of Electroless Nickel-Phosphorus Alloy Plating*, Oak Ridge Y-12 Plant Report Y-2269, Union Carbide Nuclear Co. (April 22, 1982).
10. M.S. Grewal, S.A. Sastri and B.H. Alexander, *Metal Prog.*, **91**, 98 (1974).
11. B.G. Bagley and D. Turnbull, *J. Appl. Phys.*, **39**, 5681 (1968).
12. K.S. Rajam, I. Rajagopal and S.R. Rajagopalan, *Metal Fin.*, **88**, 77 (1990).

13. B. Bozzini, P. Cavallotti, M.V. Ivanov, A. Buratti and F. Krüger, *INTERFINISH Cong.*, São Paulo, Brazil, October 1992.
14. G.O. Mallory, private communication, 10 Feb. 1995.
15. H.G. Schenzel and H. Kreye, *Plat. and Surf. Fin.*, **77**, 50 (Oct. 1990).
16. R.C. Agarwala and S. Ray, *Z. Metallkd.*, **83**(3), 199 (1992).
17. A.H. Graham, R.W. Lindsey and H.J. Read, *J. Electrochem. Soc.*, **112**(4), 401 (1965).
18. H. Kreye, H.H. Muller and T. Petzel, *Galvanotechnik*, **77**, 561 (1986).
19. W. Crook, Halliburton Industries, private communication, 26 Sept. 1979.
20. M.W. Mahoney and P.J. Dynes, *Scripta Metallurgia*, **19**, 539 (1985).
21. N.M. Martyak, S. Wetterer, L. Harrison, M. McNeil, R. Heu and A.A. Neiderer, *Plat. and Surf. Fin.*, **80**, 60 (June 1993).
22. R.N. Duncan, *AESF SUR/FIN '90, Session U*, Boston, MA (1990).
23. R. Weil, J.H. Lee, I. Kim and K. Parker, *Plat. and Surf. Fin.*, **76**, 62 (Feb. 1989).
24. V.P. Moysseyev, *Isvestija AN SSSR, Phys.*, **26**(3), 378 (1962).
25. J.P. Rankin and H.E. Hindermann, *Plating*, **54**, 523 (May 1967).
26. G.O. Mallory and Dan Altura, *Proc. 19th Ann. Airline Plat. & Metal Fin. Forum, Paper No. 830693*, San Antonio, TX, March 1983.
27. R.N. Duncan, unpublished results, 1988.
28. M.J. Aleksinas and R.C. Andre, *Metal Fin.*, **90**, 103 (June 1992).
29. P. Albert, Z. Kovac, H. Lilienthal, T. McGuire and Y. Nakamura, *J. Appl. Phys.*, **38**(3), 1258 (1967).
30. R. Bensen, Honeywell Inc., private communication, 1981.
31. W. Riedel, *op. cit.*, 152.
32. B. Jackson, R. Macary and G. Shawhan, *Trans. Inst. Met. Fin.*, **68**(3), 75 (1990).
33. Properties of Some Metals and Alloys, International Nickel Co., 1982.
34. F.L. LaQue and H.R. Copson, *Corrosion Resistance of Metals and Alloys*, Reinhold Publishing, New York, NY, 1963; p. 477.
35. R.N. Duncan, *Third AESF Electroless Nickel Symp.*, Orlando, FL 1986.

#### About the Author



*Ronald N. Duncan is vice president of Palm International, Inc., 1289 Bridgestone Parkway, Laverne, TN 37086, and is responsible for the company's technical and educational activities. Formerly, he was director of research for Elnic, Inc., where he was in charge of electroless nickel formulation and materials research. He holds a BS in mechanical and metallurgical*

*engineering from Vanderbilt University and is a registered professional engineer, and is certified as a corrosion specialist by NACE. He is the principal author of the chapter on electroless nickel in Vol. 5 of the ASM Metals Handbook.*